Translational Oncology 13 (2020) 100754

Contents lists available at ScienceDirect

Translational Oncology

journal homepage: www.elsevier.com/locate/tranon

Targeting P4HA1 with a Small Molecule Inhibitor in a Colorectal Cancer PDX Model☆

Sumit Agarwal [a], Michael Behring [a], Hyung-Gyoon Kim [a], Prachi Bajpai [a], Balabhadrapatruni V.S.K. Chakravarthi [a], Nirzari Gupta [b], Amr Elkholy [a], Sameer Al Diffalha [a], Sooryanarayana Varambally [a,c,1], Upender Manne [a,c,*,1]

[a] Department of Pathology, University of Alabama at Birmingham, Birmingham, AL 35233, USA
[b] Department of Chemistry, University of Alabama at Birmingham
[c] Comprehensive Cancer Center, University of Alabama at Birmingham

ARTICLE INFO

Article history:
Received 31 January 2020
Received in revised form 28 February 2020
Accepted 29 February 2020
Available online xxxx

ABSTRACT

Deposition, remodeling, and signaling of the extracellular matrix facilitate tumor growth and metastasis. Here, we demonstrated that an enzyme, collagen prolyl 4-hydroxylase, alpha polypeptide I (P4HA1), which is involved in collagen synthesis and deposition, had elevated expression in colorectal cancers (CRCs) as compared to normal colonic tissues. The expression of P4HA1 in CRCs was independent of patient's age, race/ethnicity, gender, pathologic stage and grade, tumor location, and microsatellite instability (MSI) and p53 status. By modulating P4HA1 with shRNA, there was a reduction in malignant phenotypes of CRCs, including cell proliferation, colony formation, invasion, migration, and tumor growth, in mice regardless of their p53 and MSI status. Immunoblot analysis of excised xenograft tumors developed from cells with silenced PH4HA1 showed low levels of proliferating cell nuclear antigen. Further, in CRC mouse models, silencing of P4HA1 in HT29 cells resulted in less metastasis to liver and bone. P4HA1 expression was regulated by miR-124, and inhibition of cell growth was noted for CRC cells treated with miR-124. Furthermore, low levels of the transcriptional repressor EZH2 reduced P4HA1 expression in CRC cells. Inhibition of P4HA1 with the small molecule inhibitor diethyl-pythiDC decreased AGO2 and MMP1, which are P4HA1 target molecules, and reduced the malignant phenotypes of CRC cells. Treatment of CRC patient-derived xenografts that exhibit high expression of P4HA1 with diethyl-pythiDC resulted in tumor regression. Thus, the present study shows that P4HA1 contributes to CRC progression and metastasis and that targeting of P4HA1 with diethyl-pythiDC could be an effective therapeutic strategy for aggressive CRCs.

Introduction

Colorectal cancer (CRC), the third most common cancer worldwide, accounts for 8% of cancer-related deaths [1]. Various environmental factors; epigenetic alterations; and gene fusions, deletions, and amplifications are involved in the initiation and progression of this complex and heterogeneous disease [2,3]. Despite recent advances in diagnostic techniques and treatment therapies, the overall survival of CRC patients remains relatively low. Hence, there is a need to identify driving genes and uncover oncogenic pathways for early detection, diagnosis, and treatment of patients with CRC.

The extracellular matrix (ECM) and its remodeling contribute to tumor pathogenesis. The tumor microenvironment is characterized by imbalances in ECM homeostasis by matrix metalloproteinases, leading to cancer progression and metastasis [4,5]. Changes in the tumor microenvironment along with ECM disruption are also a feature of CRC progression. Most proteins that are required for collagen synthesis are upregulated in CRCs and colorectal liver metastases [6]. Fragments of degraded type I, III, and IV collagen (C1M, C3M, and C4M) and type III collagen (Pro-C3) are elevated in CRCs as compared to adenomas and normal colon [7].

The prolyl-4-hydroxylase enzymes prolyl 4-hydroxylase, alpha polypeptide I (P4HA1); P4HA2; and P4HB are necessary for collagen synthesis and deposition; matrix metalloproteinases degrade collagen [8]. P4HA1 catalyzes the formation of 4-hydroxyproline from proline residues, a process that is essential for the proper folding of collagen polypeptide chains into stable triple-helical molecules [9]. Knockdown of P4HA1 inhibits neovascularization of gliomas [10].

The P4HA1/HIF1 pathway is essential for stemness of breast cancer cells, and inhibition of P4HA1 sensitizes triple-negative breast cancer cells to chemotherapy [11]. miR-30e regulates and targets P4HA1, leading to the inhibition of proliferation of hepatocellular carcinoma cells [12]. The prolyl 4-hydroxylase family members, P4HA2 and P4HA3, are overexpressed in melanomas and involved their progression [13]. For pancreatic cancer, the P4HA1-HIF1α loop has been demonstrated as a

☆ Disclosure of potential conflicts of interest: No potential conflicts of interest were disclosed.

* Address all correspondence to: Upender Manne, Ph.D., Professor and Director of Anatomic Translational Pathology, Department of Pathology, Wallace Tumor Institute, Room # 420A, University of Alabama at Birmingham, Birmingham, AL 35233, USA.
E-mail address: upendermanne@uabmc.edu. (U. Manne).

[1] Contributed equally for senior authorship.

http://dx.doi.org/10.1016/j.tranon.2020.100754

regulator of glycolysis and oncogenic activity [14]. Expression of P4HA1 and P4HA2 induces collagen deposition and promotes invasion of breast cancers, which leads to lymph node and lung metastases [8]. Our previous study showed that P4HA1 overexpression is involved in progression of prostate cancers via MMP1 [15]. P4HA1 is a prognostic marker for high-grade gliomas [16] and oral squamous cell carcinomas [17]. The only study involving P4HA1 and CRC using algorithm-based meta-analysis demonstrates that secreted P4HA1 is a potential biomarker of early diagnosis of CRC [18].

In the present study, we demonstrated an oncogenic role of P4HA1 in progression and metastasis of CRCs. There was overexpression of P4HA1 in CRCs, as compared to normal colon, regardless of tumor stage; histologic type; and patient race/ethnicity, gender, and age. Knockdown of P4HA1 decreased cell proliferation, invasion, and migration and inhibited tumor growth as well as metastases. Further, miR-124 targeted and inhibited the expression of P4HA1 in CRCs, and EZH2 regulated its expression. Inhibition of P4HA1 with 6-(5-ethoxycarbonyl-thiazol-2-yl)-nicotinic acid ethyl ester (diethyl-pythiDC) reduced the malignant phenotypes of CRC cells; tumor growth in patient-derived xenografts (PDXs); and levels of the P4HA1 downstream targets, MMP1 and argonaute 2 (AGO2). The results indicate that a P4HA1 inhibitor could be effective for therapy of CRCs.

Materials and Methods

Colorectal Tissue Specimens

Tumor specimens and matched adjacent noncancerous tissue specimens were collected from 105 patients during surgical procedures. These were provided by the Tissue Biorepository of the Anatomic Pathology Division of the University of Alabama at Birmingham (UAB). The study was conducted with prior approval of the UAB Institutional Review Board. Frozen tissues were used for RNA and protein isolation to evaluate P4HA1 expression using quantitative real-time PCR (qRT-PCR) (Supplementary Table S1) and immunoblot analysis, respectively. Formalin-fixed, paraffin-embedded archival tissue blocks containing CRCs or their corresponding normal/benign tissues were used for localization of P4HA1 by immunohistochemical (IHC) analyses.

Cell Lines and RNA Interference

CRC cell lines HCT116$^{p53\text{-}wt,MSI}$ and HCT116$^{p53\text{-}null,MSI}$ exhibit microsatellite instability (MSI), and SW480$^{p53\text{-}mut,MSS}$ cells having microsatellite stability (MSS) were grown in McCoy's medium (Corning Cellgro, Fisher Scientific Co., Pittsburgh, PA) with 10% fetal bovine serum (FBS, Invitrogen, ThermoFisher Scientific, Carlsbad, CA) in a 5% CO_2 cell culture incubator. As described earlier [15,19], lentiviruses against the *P4HA1* gene were packaged in pGreenPuro shRNA expression lentivectors (Systembio, Palo Alto, CA) by the University of Michigan Vector Core. CRC cells were infected with lentiviruses expressing P4HA1 shRNA or scramble controls, and stable cell lines were generated by selection with 1 μg/ml puromycin (Life Technologies, CA). P4HA1 shRNA sequences are listed in Supplementary Table S2. Stable cells were used for RNA isolation, immunoblot analyses, and cell-based assays.

IHC Analysis

IHC analysis was performed for CRC tissue sections as described earlier [20–22]. Briefly, sections were deparaffinized, rehydrated, antigen-retrieved, and blocked with BLOXALL Endogenous Peroxidase and Alkaline Phosphatase Blocking Solution (Cat. # SP-6000, Vector Laboratories, Burlingame, CA) for 20 minutes to remove traces of endogenous peroxidase. Subsequently, tissue sections were blocked with Normal Horse Serum Blocking Solution (Cat. # S-2012, Vector laboratories, Burlingame, CA) for 1 hour at room temperature and probed with polyclonal anti-P4HA1 antibody for 1 hour at room temperature. After washes with phosphate-buffered saline (PBS) with Tween, tissue sections were incubated for 1 hour with ImmPRESS HRP Anti-Mouse IgG (Peroxidase) Polymer Detection Kit made in horses (Cat. # MP-7401, Vector Laboratories, Burlingame, CA) as a secondary antibody. After incubation, sections were subjected to washing with PBS with Tween and PBS. Further, ImmPACT DAB Peroxidase (HRP) Substrate (Cat. # SK-4105, Vector Laboratories, Burlingame, CA) was used for color development. Slides were counterstained with hematoxylin solution (Cat. # H-3404, Vector laboratories, Burlingame, CA), dehydrated, and mounted with VectaMount permanent mounting medium (Cat. # H-5000, Vector Laboratories, Burlingame, CA).

Immunoblot Analysis

Antibodies used are listed in Table S4. All antibodies were employed at dilutions optimized in our laboratory. As described earlier [23,24], protein samples were separated on NuPAGE 4-12% Bis-Tris Midi Protein Gels, 20-well (Invitrogen, ThermoFisher Scientific, Carlsbad, CA), and transferred onto Immobilon-P PVDF membranes (EMD Millipore, Billerica, MA). The membranes were incubated for 1 hour in blocking buffer (Tris-buffered saline, 0.1% Tween, 5% nonfat dry milk), followed by incubation overnight at 4°C with the primary antibody. After three washes with Tris-buffered saline and 0.1% Tween, the blots were incubated with horseradish peroxidase–conjugated secondary antibody, and Luminata Crescendo chemiluminescence Western blotting substrate (EMD Millipore, Billerica, MA) was used as per the manufacturer's protocol for capturing signals. Signals were acquired with an Amersham Imager 600RGB (GE Healthcare Life Sciences, Pittsburgh, PA).

Cell Proliferation Assay

To assess cellular proliferation, stable P4HA1 knockdown or scramble-control CRC cells (1×10^4) were seeded in triplicate wells of 24-well plates as described [25]. After trypsinization, cell numbers were counted with a Z2 Coulter particle counter (Beckman Coulter, Brea, CA) at 2, 4, and 6 days.

Colony Formation Assay

For assay of colony formation, P4HA1-deficient or control NT shRNA-modulated CRC cells (1×10^3) were seeded in six-well plates as described previously [26]. After 10 days, cells were fixed with glutaraldehyde and stained with crystal violet. Images of representative fields were captured with an Amersham Imager 600RGB (GE Healthcare Life Sciences, Pittsburgh, PA).

Invasion Assay

To assess the involvement of P4HA1 in the malignant properties of CRC cells, cell invasion was evaluated using Corning BioCoat Matrigel invasion chambers (Cat. # 354480, Corning, NY), as described previously [27,28]. CRC cells (5×10^4 in 500 μl) with stable P4HA1 knockdown or treated with a scramble control were layered with serum-free medium on 8-μm pore inserts of Transwell membranes in triplicate; the lower chambers contained 10% FBS as a chemoattractant. After 48 hours, invaded cells were fixed and stained, and images were acquired with a phase-contrast microscope.

Wound-Healing Assay

Cell motility was assessed by a wound-healing assay, as described previously [29]. CRC cells transfected with P4HA1 shRNA or a control shRNA were seeded in triplicate on 35-mm Petri dishes. After overnight incubation, cells were serum-starved for 12 hours, and artificial wounds were created on the monolayers of confluent cells with the tip of a 200-μl pipet. At 0 and 24 hours, photographs were taken with an inverted phase-contrast microscope and a 4× objective.

3D Spheroid Model

Tests were performed to determine the spheroid-forming capacity of cancer cells using Cultrex 3D spheroid BME cell invasion assays (Cat. # 3500-096-K, Trevigen, Gaithersburg, MD), as described previously [30]. Briefly, 5000 cells were seeded in 96-well plates in triplicate with spheroid Formation ECM extract for 72 hours of incubation. An invasion matrix was added to the wells, and, after 1 hour, media supplemented with FBS were added. After 4 days, images were taken with a 4× objective.

Colorectal Cancer Xenografts

To evaluate the role of P4HA1 in tumor growth, xenografts were prepared by subcutaneously implanting CRC cells transfected with P4HA1 shRNA or control shRNA into the right dorsal flanks of 6-week-old NOD/SCID/IL2γ receptor-null (NSG) mice ($n = 7$ for each group), as described previously [22,31]. The animals were observed for tumor growth, pain, and activity following all regulatory standards in accordance with the guidelines of the University of Alabama at Birmingham Institutional Animal Care and Use Committee. Tumor length and width were measured with Vernier calipers, and tumor volumes were estimated by the following equation: $(0.52) \times (\text{length}) \times (\text{width}^2)$. At 5 weeks after implantation of CRC cells, the mice were sacrificed, and tumors were excised. The tumors were photographed and weighed.

Bioluminescence Imaging of Tumor Metastasis

For metastasis experiments, $HT29^{p53\text{-}mut}$/LUC cells (1×10^6) transfected with control NT shRNA or P4HA1 shRNA were injected into the lateral tail veins of 6-week-old NSG mice. Bioluminescent quantification was performed every 7 days for 4 weeks using IVIS Lumina III (Perkin Elmer, Waltham, MA) after intraperitoneal inoculation of 100 μl of luciferin solution (25 mg/ml). At completion of the experiment, organs were imaged for *ex vivo* luminescence.

Patient Samples and Establishment of Patient-Derived Colorectal Xenografts

Tumors and corresponding matched normal specimens were obtained from CRC patients undergoing surgery for the primary disease at UAB. Patients provided informed written consent, and samples were procured with approval of the UAB Institutional Review Board. Specimens were obtained within 4 hours of surgery and immediately transferred to media supplemented with 10% FBS. Normal colon specimens were divided into two parts: one was fixed in 10% neutral-buffered formalin, and the other was snap-frozen in liquid nitrogen. Tumor specimens were divided into fragments of approximately 3×3 mm^2 for subcutaneous implantation into 6- to 7-week-old NSG mice; the remainder was either fixed in 10% neutral-buffered formalin or snap-frozen in liquid nitrogen. Following implantation of the fragments, mice were monitored for tumor growth. For expansion of the model, xenografted tumors were implanted into mice for several passages; one of the passages was used for treatment with diethyl-pythiDC. When tumor sizes reached 200 mm^3, the mice ($n = 2$) were injected intraperitoneally with diethyl-pythiDC at 100 mg/kg once per week for 6 weeks. Control mice ($n = 2$) were dosed with the vehicle. Tumor sizes were measured with calipers.

Statistical Analysis

For paired samples, differences in IHC scores between tumor and normal tissue were evaluated using a paired Wilcoxon signed-rank test. A secondary analysis of effect modification for paired tumor normal IHC scores was accomplished using the same test for the following covariates: stage, gender, race, age, MSI status, and any p53 somatic mutation. For experiments with cell lines, Student's *t* test was used to perform comparisons of mean values. A *P* value of less than .05 was considered statistically significant.

Results

P4HA1 Gene Overexpression in CRCs

Datasets available from Kaiser et al. (2007) [32] (Figure 1*A*), TCGA 2012 [33] (Figure 1*B*), and Skrzypczak et al. (2010) (Supplementary Figure S1*A*) showed P4HA1 overexpression in colon adenocarcinomas as compared to normal colon tissues. Kaiser et al. (2007) (Supplementary Figure S1*B*) and TCGA (2012) (Supplementary Figure S1*C*) showed overexpression in mucinous adenocarcinoma. P4HA1 expression in TCGA RNA-seq dataset accessed using the UALCAN online data portal [34] (http://ualcan.path.uab.edu/) showed P4HA1 upregulation in CRCs ($n = 286$) as compared to normal cancer tissues ($n = 41$) (Figure 1*C*). Quantitative PCR, performed to confirm the differential expression of P4HA1 in CRC tissues ($n = 105$) as compared to matched noncancerous tissues ($n = 105$), showed overexpression of P4HA1 in CRCs (Figure 1*D*). As determined with UALCAN, P4HA1 expression in various stages of CRC (Figure 1*E*) and patient's race (Figure 1*F*) was upregulated. These data were validated by qPCR analysis of paired samples of different stages [Stage 1 ($n = 18$), Stage 2 ($n = 29$), Stage 3 ($n = 41$), and Stage 4 ($n = 17$)] (Figure 1*G*) and patient's race [Caucasian ($n = 75$) vs African-American ($n = 22$)] (Figure 1*H*). For all stages, there was overexpression of P4HA1 ($P < .001$) as compared to the matched normal colon tissues. As established with UALCAN, there was upregulated expression of P4HA1 across tumor histotypes (Supplementary Figure S2*A*) and patient's gender (Supplementary Figure S2*B*) and age (Supplementary Figure S2*C*). Further, qPCR analysis showed that overexpression of P4HA1 was independent of tumor histotype [adenocarcinoma ($n = 88$); mucinous adenocarcinoma ($n = 17$)] (Supplementary Figure S2*D*), gender [male ($n = 53$) vs female ($n = 52$)] (Supplementary Figure S2*E*), and age [21-40 years ($n = 4$), 41-60 years ($n = 29$), 61-80 years ($n = 55$), and 81-100 years ($n = 17$)] (Supplementary Figure S2*F*). These data showed P4HA1 RNA overexpression in CRCs as compared to normal colon. In sum, P4HA1 RNA expression was independent of tumor stage and histotype as well as patient's race, age, and gender.

P4HA1 Protein Upregulation in CRC

After confirming RNA overexpression in CRC, we investigated for P4HA1 protein expression in CRC tissues and corresponding noncancerous tissues using immunoblot analysis and found overexpression of P4HA1 in CRC tissues (Figure 2*A*). Further, we performed immunohistochemical analysis to investigate for localization of P4HA1 in tissue specimen containing CRC as well as normal colon and found overexpression of P4HA1 in cytoplasm as compared to normal colon (Figure 2*B*). Furthermore, covariates of gender, age, stage, race, MSI, and p53 somatic mutation status were found to have no effect upon this increase in tumor IHC as compared to normal (Supplementary Table S1). Tumor samples had consistently higher IHC scores than their paired normal (Wilcoxon paired *P* value $< .001$) (Figure 2*C*), regardless of tumor stage (Figure 2*D*), patient's race (Supplementary Figure 3*A*), gender (Supplementary Figure 3*B*), and age (Supplementary Figure 3*C*). These findings suggest that P4HA1 is a reliable marker of tumor tissue in the real world with CRC of various stages and molecular characteristics. These data also showed P4HA1 protein overexpression in CRC suggesting that P4HA1 could be involved in the progression of CRC.

CRC Growth Inhibition After P4HA1 Knockdown Is Independent of p53 and Microsatellite Status

To elucidate the function of P4HA1 in regulating the malignant phenotypes of CRC cells, cells were stably transfected with either of two P4HA1 shRNAs. Immunoblot analysis confirmed the knockdown of P4HA1 in $HCT116^{p53\text{-}wt,MSI}$, $HCT116^{p53\text{-}null,MSI}$ and for $SW480^{p53\text{-}mut,MSS}$ (p53 mutated) cells (Figure 3*A*). After 6 days of treatment, there was lower cell growth ($P < .01$) as compared to cells transfected with control shRNA

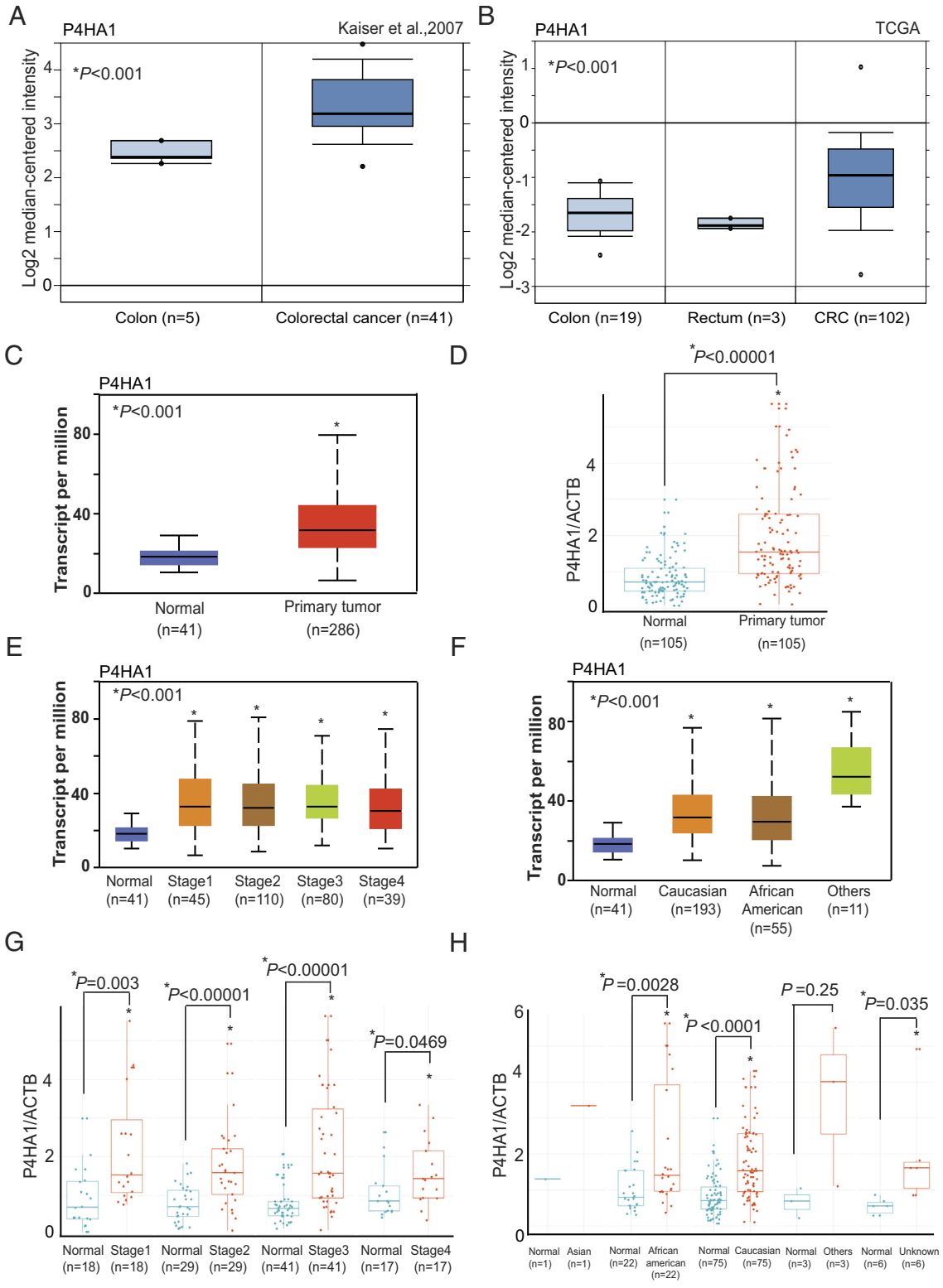

Figure 1. Overexpression of P4HA1 mRNA in CRCs. (A) Differential expression of P4HA1 between normal colon ($n = 5$) and CRC tissues ($n = 41$), as demonstrated in the Kaiser et al. (2007) colon dataset. (B) TCGA dataset showing P4HA1 expression in CRCs ($n = 102$), colon ($n = 19$), and rectum ($n = 3$). (C) TCGA data procured from UALCAN to show P4HA1 RNA expression in control ($n = 41$) and CRC ($n = 286$). (D) Mean values for P4HA1 mRNA expression for 105 cases of CRC with corresponding normal colon tissues. A paired-samples *t* test showing higher P4HA1 mRNA expression in cancer tissues compared with normal tissues ($P < .00001$). (E) Box-whisker plot showing expression of P4HA1 mRNA in CRCs based on various cancer stages from the UALCAN database. (F) Transcriptional levels of P4HA1 expression in normal individuals of any ethnicity or in CRC patients of Caucasian ($n = 193$), African-American ($n = 55$), or Asian ethnicity ($n = 11$). (G) qPCR analysis validating TCGA data in matched normal and CRC tissues with respect to stages [Stage 1 ($n = 18$), Stage 2 ($n = 29$), Stage 3 ($n = 41$), and Stage 4 ($n = 17$)]. (H) P4HA1 mRNA expression in CRCs of Caucasian ($n = 75$) *versus African-American* ($n = 22$) *patients with paired adjacent noncancerous tissues as analyzed by qPCR.*

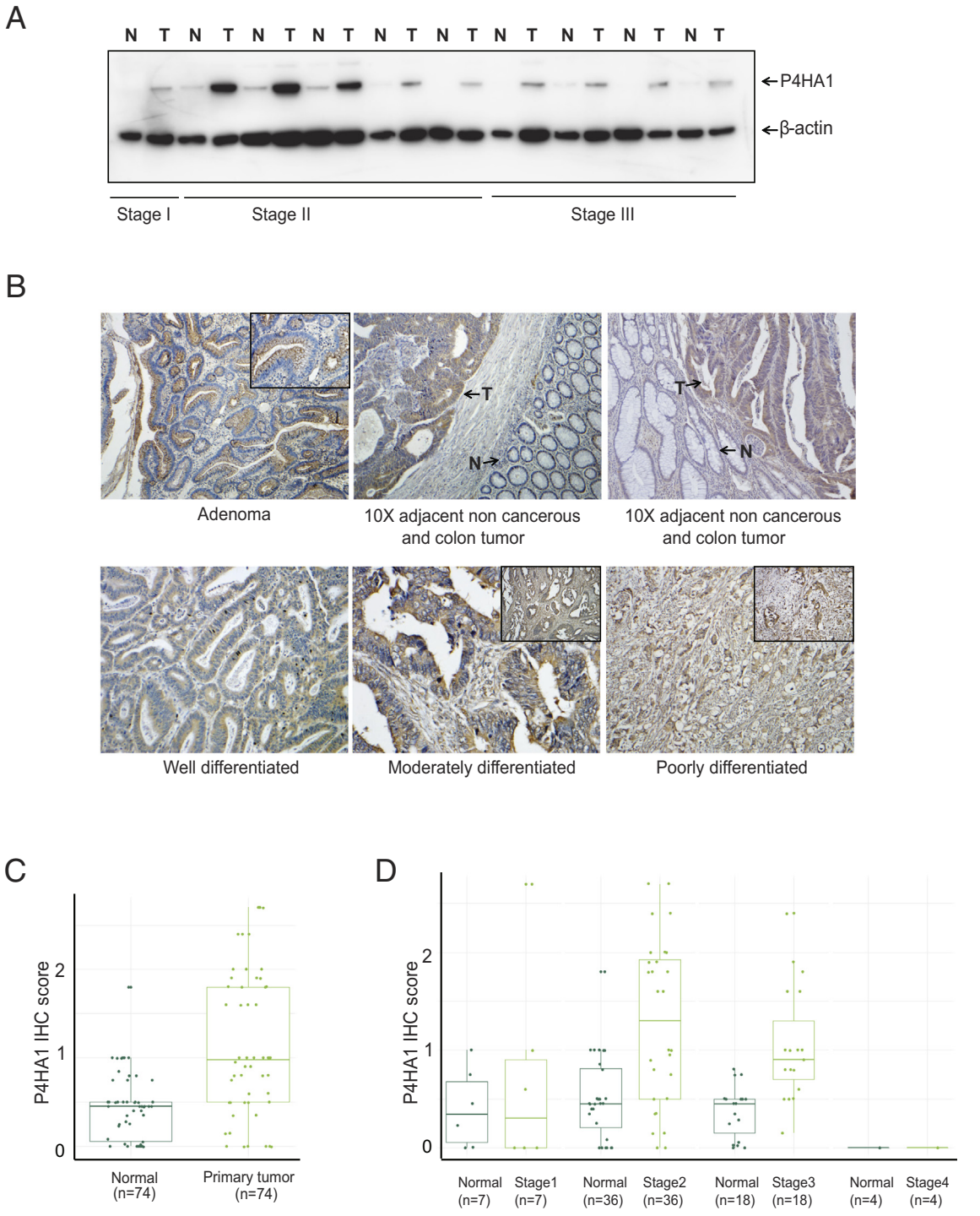

Figure 2. The P4HA1 protein is upregulated in CRCs. (A) Immunoblot analysis assessing P4HA1 protein expression in CRC tissues and corresponding normal colon tissue. (B) IHC analysis showing elevated cytoplasmic reactivity in CRC tissues compared to normal colon tissue. (C) Representative graphs of immune-reactive score after P4HA1 staining using IHC to show P4HA1 protein expression in 74 CRC patients and (D) stage-wise protein expression.

(Figure 3*B*). Colony formation assays, which determine the capacity of cancer cells to grow and accumulate into groups, were also performed. The colony-forming capacity of the CRC cells was lower for cells transfected with P4HA1 shRNA compared to cells transfected with a control shRNA (Figure 3*C*).

Further, we accomplished Transwell invasion assays, which assess the capacity of tumor cells to overcome barriers of the ECM and spread into surrounding tissue. We used Boyden chambers with 8-μm filters coated with an artificial ECM and added CRC cells transfected with P4HA1 shRNA or control shRNA to the chambers without FBS; FBS was added in the lower portion as a chemoattractant. After 48 hours, fixed and stained cells transfected with control shRNA that passed through the filters and invaded across the ECM showed high invasive potential as compared to cells transfected with an P4HA1 shRNA (Figure 3*D*).

Wound-healing assays demonstrate the migration capacity of cancer cells and show their capacity for healing of wounds. This assay showed that the closing rates for artificially created wounds in confluent cell populations were lower for P4HA1-deficient cells as compared to cells

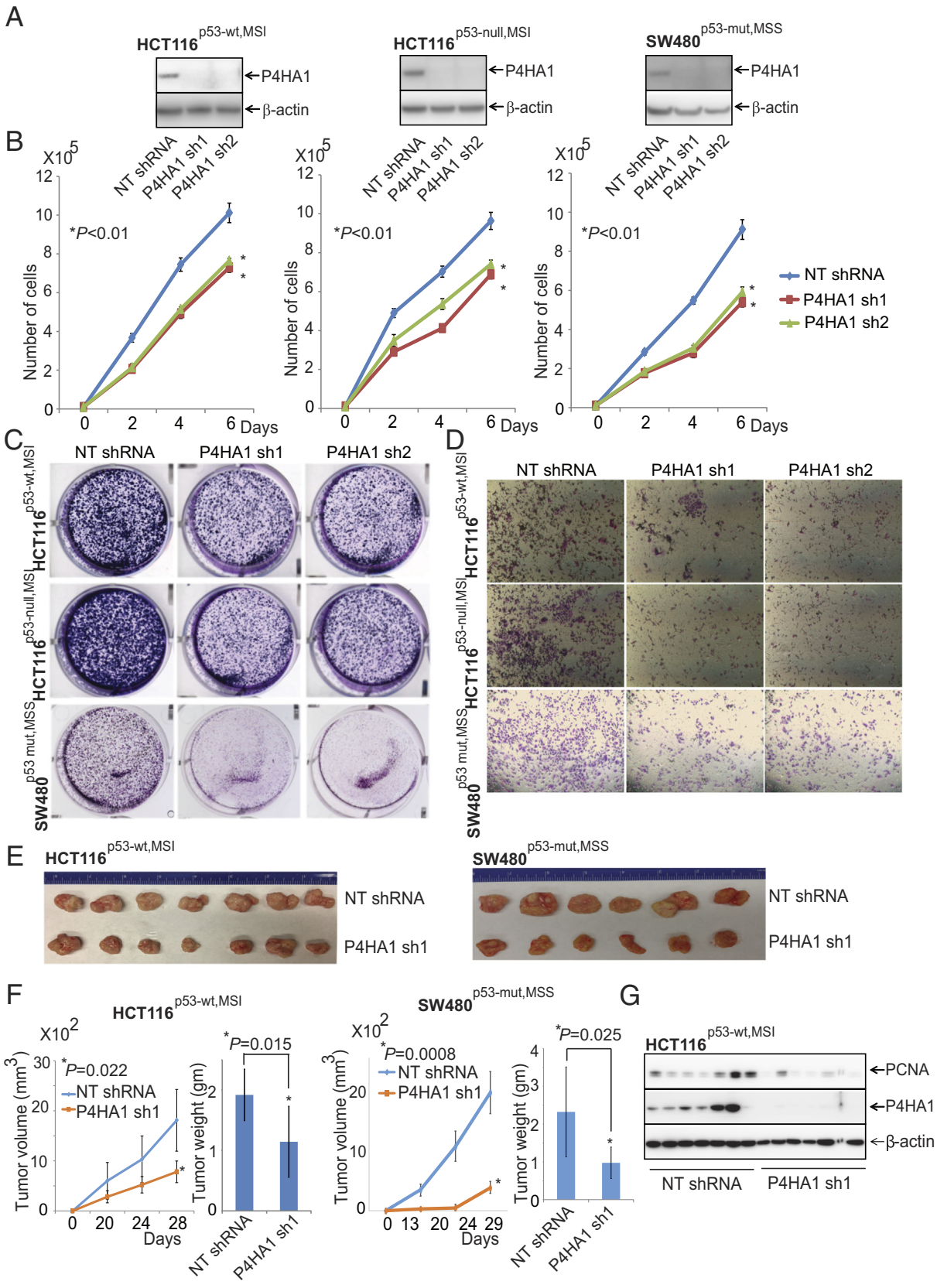

Figure 3. P4HA1 knockdown reduces malignant phenotypes of CRC cells. (A) Immunoblot analysis showing P4HA1 knockdown efficiency in CRC cells HCT116$^{p53\text{-}wt,MSI}$ and HCT116$^{p53\text{-}null,MSI}$ and for SW480$^{p53\text{-}mut,MSS}$. (B) Proliferation of CRC cells following P4HA1 knockdown in comparison with control NT shRNA, as determined by cell counting at 2, 4, and 6 days. (C) Colony formation assay showing the effect of P4HA1 knockdown. (D) Transwell cell invasion assays showing the invasion potential of P4HA1 knockdown and control NT-shRNA CRC cells. (E) Representative photograph showing excised tumors from mice implanted with HCT116 or SW480 cells. (G) Volumes and weights of HCT116$^{p53\text{-}wt,MSI}$ and SW480$^{p53\text{-}mut,MSS}$ xenograft tumors shown in histographs. (H) Immunoblot analysis of levels of P4HA1 and PCNA in P4HA1-knockdown and control shRNA groups.

transfected with control shRNA (Supplementary Figure 3). These results suggest that P4HA1 is involved in the malignant properties of CRCs.

To investigate the role of P4HA1 in tumor growth, we established CRC xenografts in NSG mice. For this purpose, we subcutaneously implanted, into the right dorsal flanks of mice, 1 million HCT116$^{p53\text{-}wt}$ or SW480$^{p53\text{-}mut}$ cells transfected with a control shRNA or a P4HA1 shRNA. Consistent with the results obtained from cell culture assays, knockdown of P4HA1 suppressed the growth of HCT116$^{p53\text{-}wt,MSI}$, and SW480$^{p53\text{-}mut,MSS}$ CRC xenografts (Figure 3*E*). With P4HA1 knockdown, there were lower volumes and weights of HCT116$^{p53\text{-}wt}$ and SW480$^{p53\text{-}mut}$ tumors as compared to cells transfected with control shRNA (Figure 3*F*). In lysates of HCT116$^{p53\text{-}wt,MSI}$ xenograft tumors, protein levels of P4HA1 and PCNA were lower for those with P4HA1 knockdown than in those from cells transfected with control shRNA (Figure 3G). These data showed the role of P4HA1 in CRC progression and tumor growth and CRC growth inhibition after P4HA1 knockdown is independent of p53 and MSI status.

miR-124 Targets and Downregulates P4HA1 Expression in CRCs

Previous studies of our laboratory using the microRNA prediction web tools TargetScan, miRanda, and miRSearch V3.0 identified miR-124 as potentially targeting P4HA1 [15]. Figure 4*A* shows the binding sites of miR-124 to 3′-UTR of P4HA1. By co-transfecting HEK-293 cells with miR-124 and pMir-REPORT-P4HA1 3′-UTR plasmids, we showed, by employing a 3′-UTR assay, that miR-124 regulates P4HA1 [15]. These co-transfections reduced luciferase reporter activity compared to transfection with a control-miR. In addition, lower luciferase activity was evident when the pMir-REPORT-P4HA1 3′-UTR plasmid had a mutated miR-124 target site, indicating that miR-124 regulates and binds to P4HA1 [15].

In the present study, we performed transfections to determine whether miR-124 targets and suppresses the expression of P4HA1 in HCT116$^{p53\text{-}wt,MSI}$ CRC cells. Immunoblot analyses demonstrated that forced expression of miR-124 decreased the expression of P4HA1 relative to a nontargeting control miRNA (Figure 4*B*). To assess the functional significance of miR-124 in CRCs, we overexpressed it in HCT116 cells and found less cell proliferation (Figure 4*C*), colony formation (Figure 4*D*), and migration (Figure 4*E*). These results suggest the role of miR-124 in targeting the expression of P4HA1 in CRC cells.

EZH2 Regulates P4HA1 Expression in CRCs

A previous study from our laboratory showed that, in prostate cancers, the transcriptional repressor EZH2 regulates the expression of P4HA1 [15]. For the present study, we hypothesized that, in CRCs, EZH2 also regulates P4HA1. Knockdown of EZH2 in HCT116$^{p53\text{-}wt,MSI}$, SW480$^{p53\text{-}mut,MSS}$, and HT29$^{p53\text{-}mut,MSS}$ cells lowered their P4HA1 levels (Figure 4*F*). Expression of H3K27me3, a mark of EZH2-mediated trimethylation of histone H3 on lysine 27, is lower when CRC cells are exposed to EZH2 shRNA (Figure 4*F*). Overexpression of EZH2 in CRL1807 SV40-transformed colon cells increased the expression of P4HA1 as compared to controls, but the SET domain mutant EZH2 (EZH2ΔSET) repressed P4HA1 expression (Figure 4*G*). This suggests that EZH2 regulates the function of P4HA1 in CRC cells and its regulation is independent of the p53 and microsatellite status.

P4HA1 Is Involved in CRC Metastasis

To establish, with mice, the contribution of P4HA1 to metastasis, we performed tail-vein injections of luciferase-expressing HT29$^{p53\text{-}mut,MSS}$ cells with or without P4HA1 knockdown, and luminescence was monitored weekly. The knockdown efficiency of P4HA1 in HT29$^{p53\text{-}mut,MSS}$ cells was confirmed by Western blot analysis (Figure 5*A*). The results showed similar bioluminescent signals for lungs of both groups, but signals were enhanced in livers in control animals (Figure 5*B*). Lungs and liver are the primary metastatic sites of CRC tumors, while bone marrow metastasis reflects a widespread disease [35]. In addition, at 28 days after lateral tail-vein injections of HT29$^{p53\text{-}mut,MSS}$ CRC cells transfected with control shRNA, more colonies were evident in bones of mice as compared to those injected with P4HA1-knockdown cells. *Ex vivo* measurements of luminescence confirmed less luminescence in hind-limb bones and liver of those bearing P4HA1-knockdown cells (Figure 5*C*). Further, the contents of marrow were flushed from bones and placed in puromycin selection media for growing only cancer cells. The cells were grown for 4 days; only cells transfected with NT shRNA grew (Figure 5*D*). Hematoxylin and eosin (H&E) staining of bone sections of mice showed that mice with P4HA1 knockdown cells had less dissemination of CRC cells to bone (Figure 5*E*). Further, we assessed the interaction of CRC cells with bone marrow using cytokeratin 8/18 as a marker of cancer cells and alkaline phosphatase as a marker of bone marrow cells. There was strong staining of cytokeratin 8/18 in cells transfected with NT shRNA with limited alkaline phosphatase staining (bone marrow) as compared to HT29$^{p53\text{-}mut,MSS}$ CRC cells with P4HA1 knockdown (Figure 5*F*). These results indicate that, in this model, P4HA1 promotes CRC metastasis and knockdown of P4HA1 reduces dissemination of tumor cells to distant organs.

P4HA1 Correlates with P4HA2 and P4HB

Collagen prolyl-hydroxylases have alpha (P4HA1, P4HA2 and P4HA3) and beta (P4HB) subunits. Gene coexpression analysis of data acquired from UALCAN [34] showed a correlation of P4HA1 with P4HA2 (correlation coefficient value, CC = 0.53) and P4HB (CC = 0.55) (Supplementary Figure 5*A*). We found lower levels of P4HA2 and P4HB in CRC cells with P4HA1 knockdown (Supplementary Figure 5*B*). Exposure of cancer cells to diethyl-pythiDC decreased P4HA2 and P4HB levels (Supplementary Figure 5*C*), indicating that, in CRCs, P4HA1 correlates with isoforms of prolyl-4-hydroxylases.

Diethyl-pythiDC, a Small Molecule Inhibitor of P4HA1, Inhibits CRC Growth

Diethyl-pythiDC, a biheteroaryl compound, inhibits collagen biosynthesis in breast cancer cells [36]. In the present study, CRC cells, HCT116$^{p53\text{-}wt,MSI}$, and SW480$^{p53\text{-}mut,MSS}$ were treated with various concentrations of diethyl-pythiDC. In prostate cancers, MMP1 is a downstream target of P4HA1 [15]. After treatment of the three types of cells with diethyl-pythiDC, there was lower expression of MMP1 (Figure 6*A*). P4HA1 reduces the stability of AGO2, a molecule involved in tumorigenesis, in a miRNA-dependent manner [37,38]. Treatment of CRC cells with diethyl-pythiDC decreased levels of AGO2 (Figure 6*A*). Also, it reduced the malignant phenotypes of CRC cells, including cell proliferation (Figure 6*B*), colony formation (Figure 6*C*), invasion (Figure 6*D*), and spheroid-forming capacity (Figure 6*E*). The pythiDC treatment decreased the spheroid-forming capacity of HCT116$^{p53\text{-}wt,MSI}$ and SW480$^{p53\text{-}mut,MSS}$ cells, and the change is statistically significant; HCT116$^{p53\text{-}wt,MSI}$ (Student's t test, $P = .0002$) and SW480$^{p53\text{-}mut,MSS}$ (Student's t test, $P = .001$) (data not shown).

Diethyl-pythiDC Reduces Tumor Growth in a PDX Model of CRC

To evaluate the antitumor efficiency of diethyl-pythiDC in PDX models, the inhibitor was administered to mice bearing PDXs derived from a CRC patient. CRC tissues from the patient and the xenograft tissue were analyzed by H&E staining, which showed that CRC PDX tissues exhibited a similar histologic phenotype to that of patient tissue from which they were derived (data not shown). This PDX model of CRC was selected for treatment with diethyl-pythiDC, as it had high P4HA1 expression. Diethyl-pythiDC (100 mg/kg) inhibited tumor growth in comparison to controls (Figure 7, *A* and *B*). Further, treatment of PDXs with diethyl-pythiDC decreased the P4HA1 downstream target, MMP1 (Figure 7*C*). These results show that diethyl-pythiDC reduces growth in a CRC PDX model through the P4HA1 downstream targets, MMP1 and AGO2.

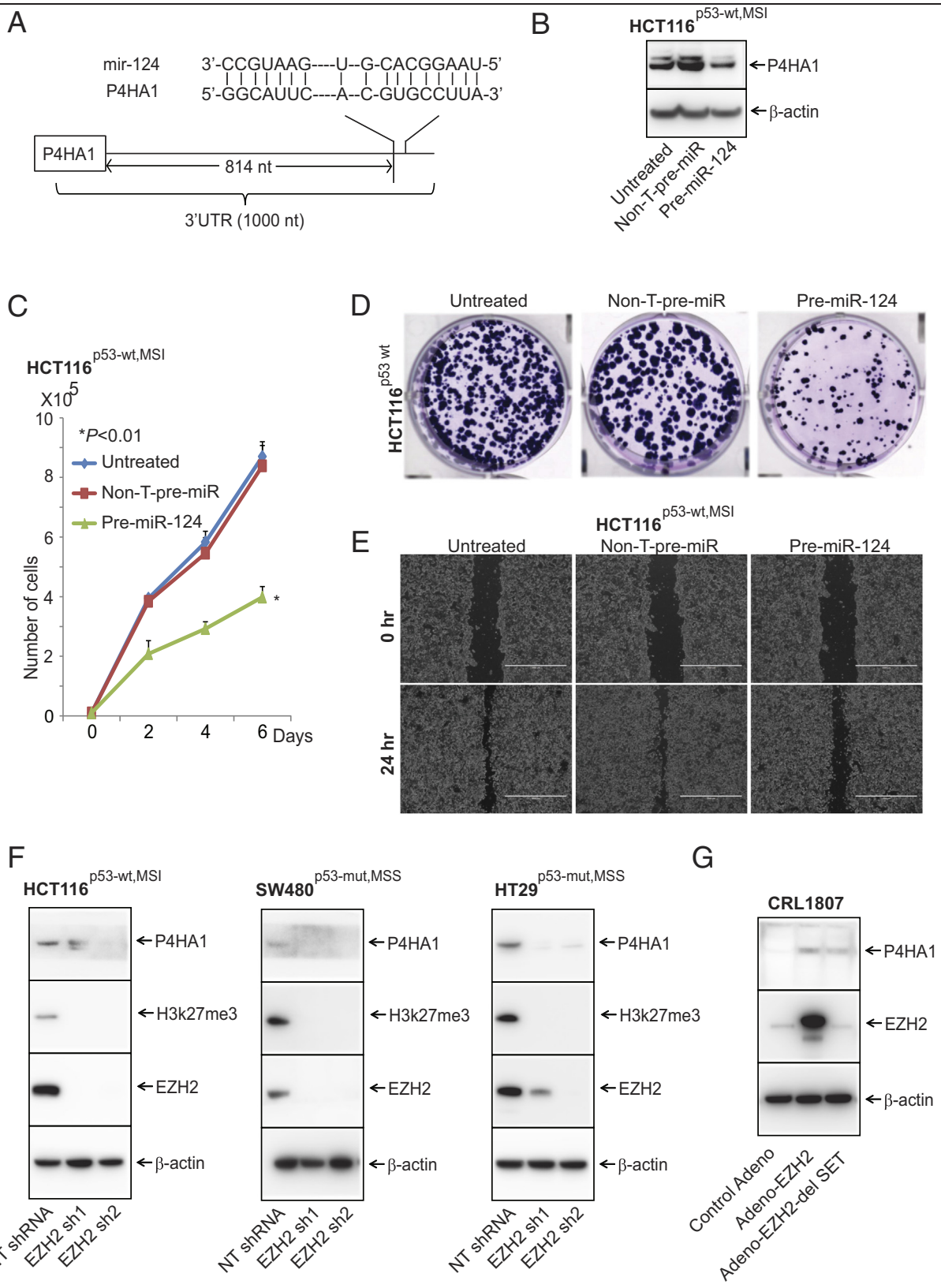

Figure 4. miR-124 and EZH2 regulate P4HA1 in CRCs. (A) Predicted binding site of miR-124 in the 3′UTR of P4HA1. (B) Immunoblot analysis showing P4HA1 expression after transfecting HCT116$^{p53\text{-}wt,MSI}$ cells with miR-124 or NT-miR. Overexpression of miR124 was accomplished, and cell proliferation (C), colony formation (D), and migration (E) assays were performed. (F) P4HA1 expression was analyzed by Western blotting in the shRNA-mediated knockdown of EZH2 in HCT116$^{p53\text{-}wt,MSI}$, SW480$^{p53\text{-}mut,MSS}$, and HT29$^{p53\text{-}mut,MSS}$ cells. Decreased repressive marks of H3K27me3 show the efficiency of EZH2 shRNA. (G) CRL1807 SV40 transformed colon cells infected with lacZ adenovirus or EZH2 or EZH2-deleted SET mutant adenovirus for 48 hours, followed by measurement of P4HA1 expression using immunoblot analysis.

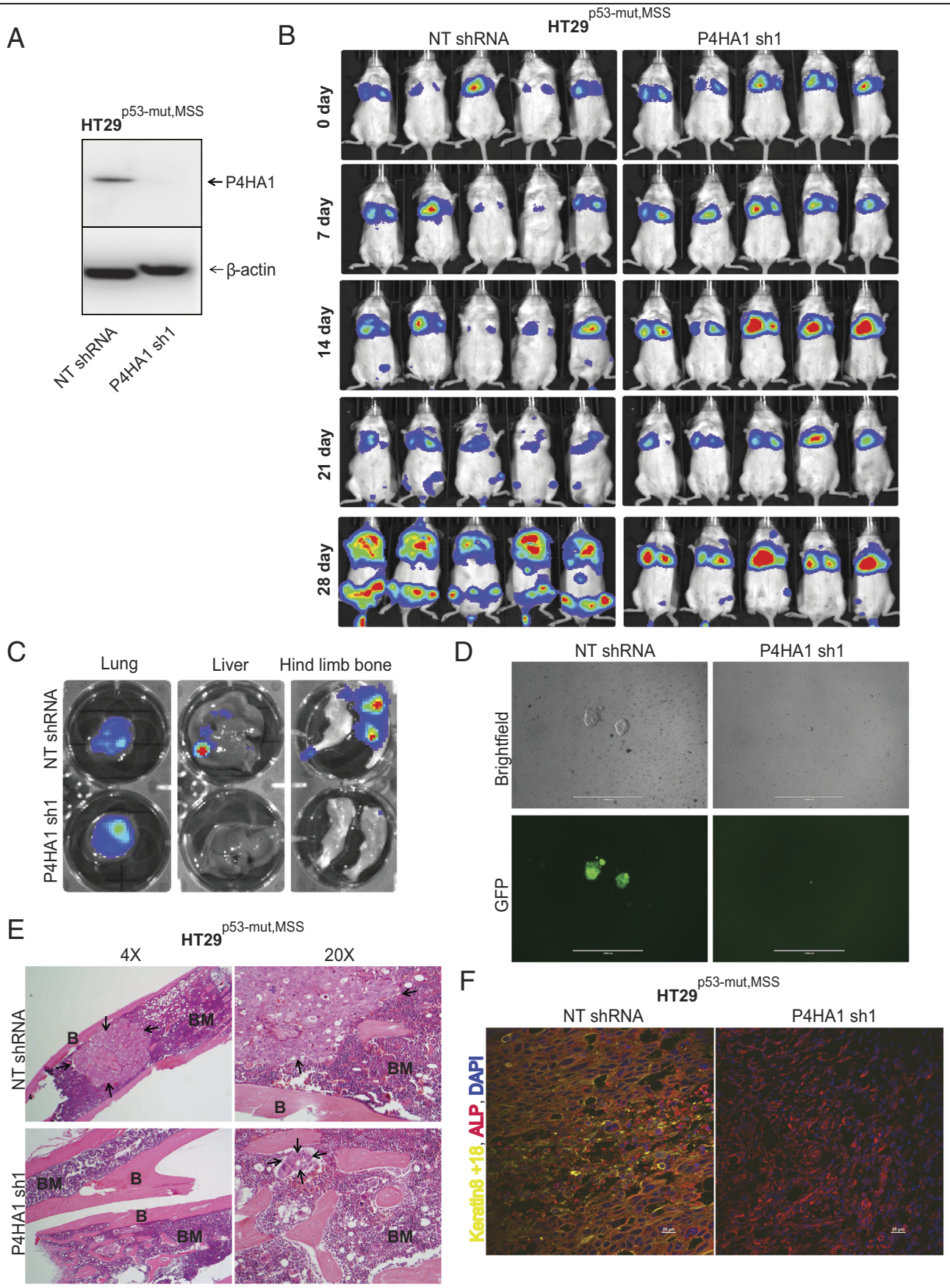

(caption on next page)

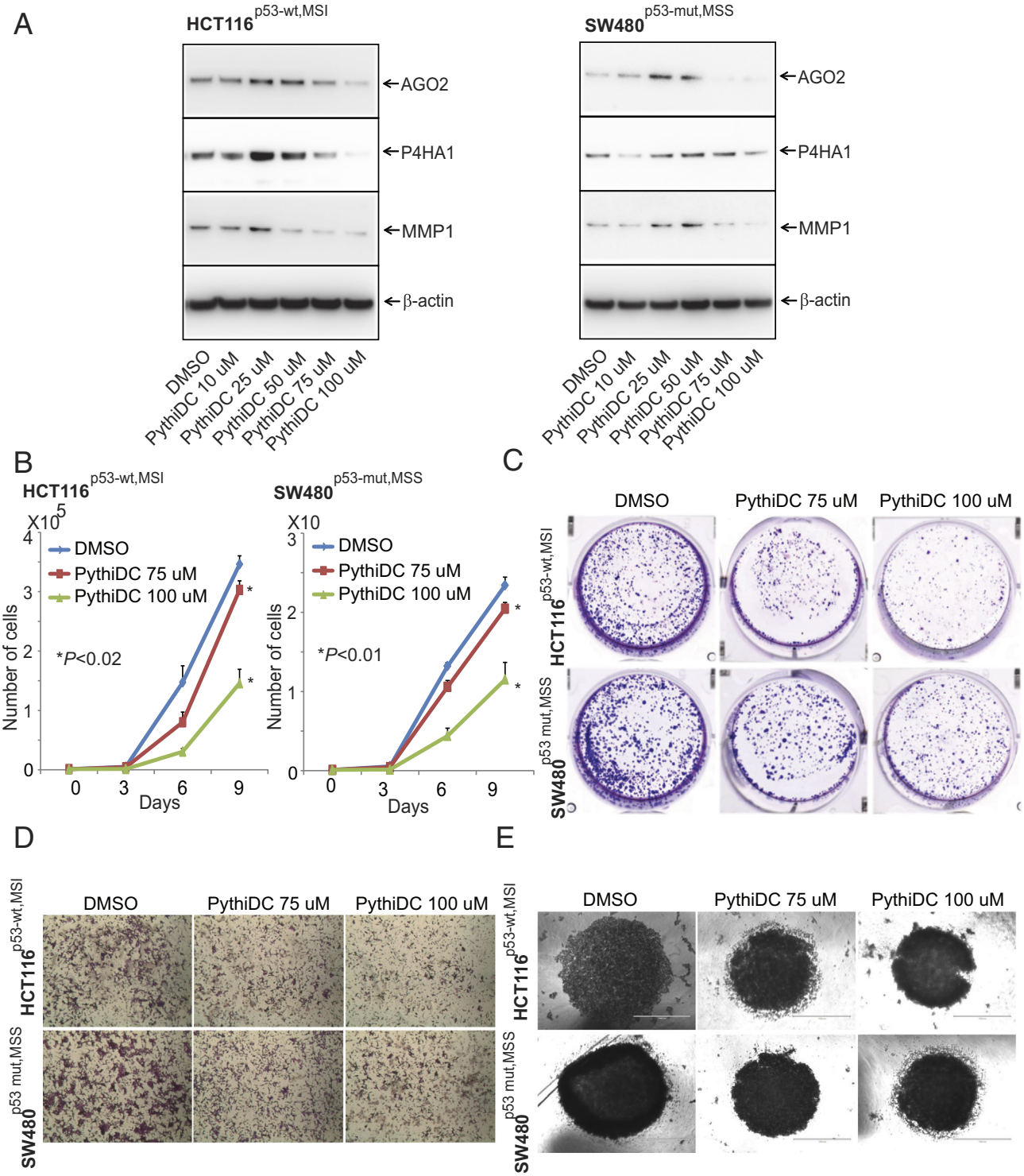

Figure 6. Treatment with the P4HA1 inhibitor, diethyl-pythiDC, impedes CRC cell growth. (A) Analysis of P4HA1, MMP1, and AGO2 protein levels using immunoblots for CRC cells treated with diethyl-pythiDC. (B) Cell proliferation assay showing the proliferation of CRC cells treated with diethyl-pytiDC. (C) Clonogenicity assay showing the colony-forming potential of CRC cells treated with diethyl-pytiDC. (D) Transwell invasion assays assessing the invasion of CRC cells in response to treatment with diethyl-pytiDC.

← **Figure 5.** P4HA1 knockdown decreases CRC tumor growth and metastasis in a xenograft model. (A) Knockdown efficiency of P4HA1 in HT29$^{p53\text{-}mut,MSS}$. (B) Bioluminescence detection of metastasis in NSG mice at indicated time points after lateral tail-vein injection of HT29$^{p53\text{-}mut,MSS}$ expressing LUC cells with or without P4HA1 knockdown. (C) At the completion of experiment, luciferin was injected to mice followed by organ excision. *Ex vivo* luminescence was performed for hind-limb bone, liver, and lungs. (D) Representative figures to show cultures of bone marrow isolated from bones of animals and cultured in puromycin-selection media; 1000 μm. (E) H&E to show the disseminated tumor cells in bones. (F) Immunofluorescence staining of bone with ALP as a marker of osteoclast lineage (red), keratin 8 + 18 as a marker of cancer cells (yellow), and DAPI for nuclear stain (blue); scale bar, 20 μm.

Discussion

Synthesis, deposition, and degradation of the ECM promote cancer progression and metastasis [39]. The present study investigated the role of P4HA1 expression in CRC progression. There was overexpression of P4HA1 in CRCs as compared to matched adjacent noncancerous tissues, and the expression was independent of the pathologic stage; histologic type; MSI or p53 status; and patient race, gender, or age. Since, in CRCs,

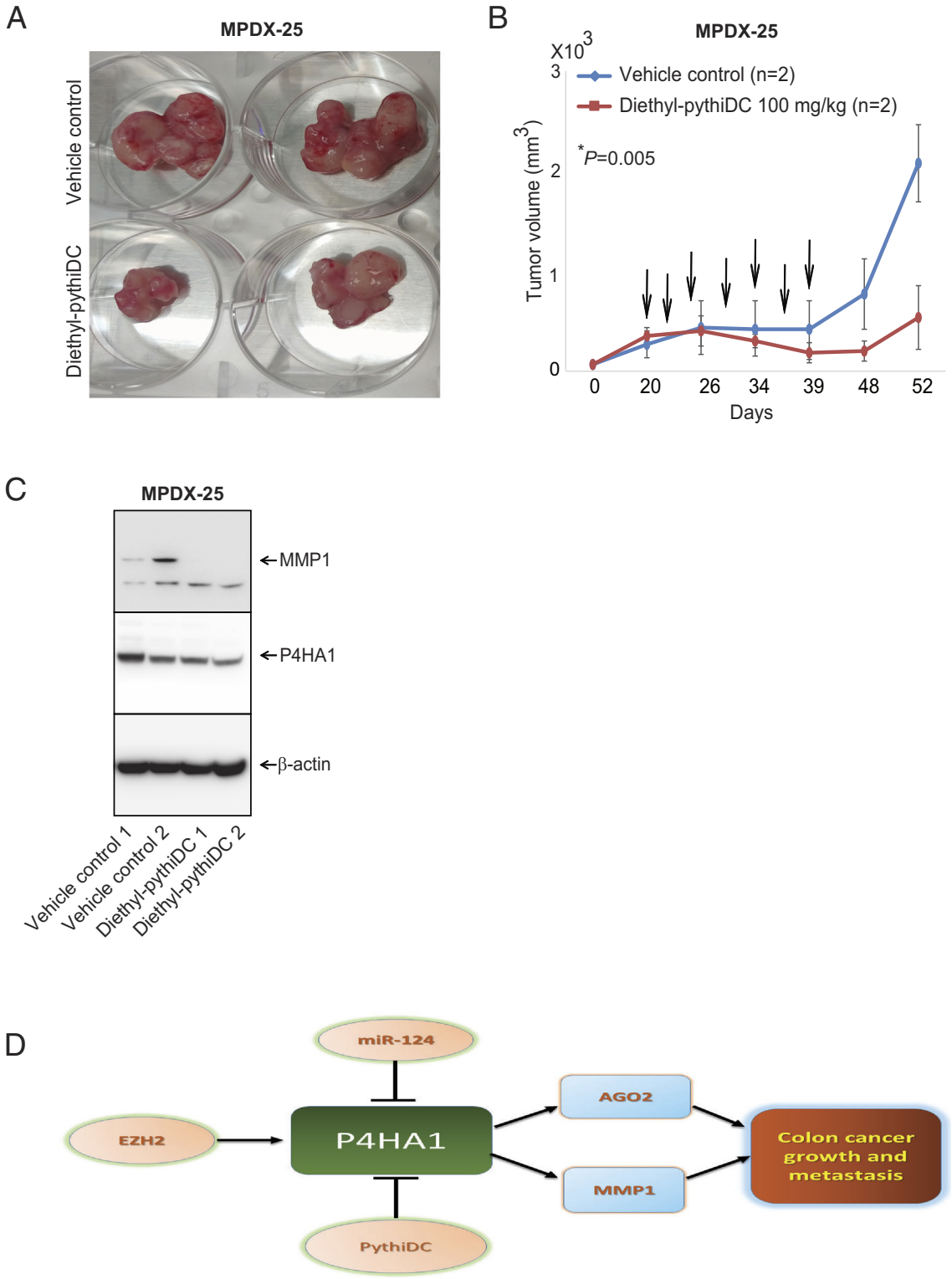

Figure 7. Diethyl-pythiDC reduces tumor growth of CRC PDXs. CRC PDX xenografts were developed in NSG mice and divided into two groups: treatment with control vehicle ($n = 2$) and treatment with diethyl-pytiDC ($n = 2$). Mice were treated once weekly for 6 weeks, and tumor size was monitored. (A) Representative photograph of excised tumors from PDXs treated with the control or diethyl-PytiDC. Arrows indicate treatment of the control and diethyl-pytiDC. (B) Tumor volumes were plotted (*$P = .005$). (C) Tumor lysates from PDXs were prepared, and immunoblot analyses were performed by probing for P4HA1 and MMP1. β-Actin was used as a loading control. (D) Proposed model of EZH2/P4HA1/MMP1 axis in CRC growth. EZH2 and miR-124 regulate P4HA1, which further regulates MMP1 and AGO2 in CRC progression and metastasis. Diethyl-pythiDC inhibits P4HA1 target molecules, MMP1 and AGO2.

p53 mutations are common (more than 50%), we assessed whether abnormal expression of P4HA1 is associated with p53 in CRC cell lines. Microsatellite (MS) instability is a molecular feature that determines the aggressiveness of CRC progression. Based on the MS status, CRCs are categorized into two molecular subtypes: those with MSI and those that are microsatellite stable (MSS). MSI-CRCs have a dysfunction of the mismatch repair genes and are less aggressive; MSS-CRCs, accounting for 85% of sporadic CRCs, have active mismatch repair genes and are more aggressive. Thus, for this study, we utilized CRC cell lines with different p53 and microsatellite status. HCT116$^{p53\text{-}wt}$ and HCT116$^{p53\text{-}null}$ cells exhibit MSI, and SW480$^{p53\text{-}mut}$ cells exhibit MSS. Inhibition of P4HA1 by an shRNA decreased migration and invasion of CRC cells and xenograft tumor growth in a manner that was not dependent on the p53 and microsatellite status of the cells. In addition, inhibition by diethyl-pythiDC decreased tumor growth in a CRC PDX model. Further, knockdown of P4HA1 decreased CRC metastasis in mice, particularly tumor cell dissemination to liver and bone. Thus, these findings provide evidence for an oncogenic role of P4HA1 in CRC progression regardless of p53 and MS status.

Invasive and motile cancer cells enter the circulatory system and infiltrate distant organs. The infiltrated cancer cells are called disseminated tumor cells [40]. Bone marrow harbors CRC disseminated tumor cells, which are a predictor of metastasis not only to bone but also to the liver and lungs [41]. The current study, which investigated, with an experimental mouse model, the functional role of P4HA1 in CRC metastasis, showed that knockdown of P4HA1 in CRC cells decreased the dissemination of these cells to the liver and bone, indicating a role for P4HA1 in CRC dissemination, metastasis, and colonization of tumor cells in distant organs.

Furthermore, we treated CRC cells with the small molecule inhibitor of P4HA1, diethyl-pythiDC [36], which decreased the malignant phenotypes of CRC cells. This inhibition of P4HA1 was consistent with a previous finding, which showed inhibition of proliferation and spheroid formation capacity of melanoma cells treated with diethyl-pythiDC [13].

PDX models mimic human cancers and effectively predict tumor responses in humans [42]. NSG mice, the favored hosts, allow high-engraftment rates of PDX CRC tissues as they, to avoid xenograft rejection, lack T, B, and functional NK cells as well as both alleles of the IL2 receptor common gamma chain [43]. The present study evaluated the effect of diethyl-pythiDC on a PDX model, established in NSG mice that expressed high levels of P4HA1. Diethyl-pythiDC treatment of mice decreased growth of CRC PDXs and expression of the MMP1 protein, a downstream target of P4HA1. These findings show that diethyl-pythiDC inhibits growth of CRCs and that, through MMP1, P4HA1 is involved in tumor progression.

As reported for prostate cancer, the transcriptional regulator EZH2, which methylates lysine 27 of histone H3 (H3K27me3) to promote transcriptional silencing, regulates P4HA1 activity [15]. For prostate cancer under hypoxia, HIF1α upregulates EZH2 expression, and EZH2 regulates P4HA1 expression by repressing miR-124 [15]. In the present study, silencing of EZH2 in CRC cells by shRNA knockdown decreased expression of the P4HA1 protein. Also, for CRC cells, overexpression of EZH2 by adenovirus infection increased expression of the P4HA1 protein, showing that it regulates P4HA1 expression.

MiRNAs, small noncoding nucleotides, can function either as oncogenes or tumor suppressors. miR-124 acts as a tumor suppressor and is epigenetically silenced in gastric cancer [44], breast cancer [45], and nasopharyngeal carcinoma [46]. A previous study from our laboratory shows that, in prostate cancer cells, miR-124 regulates and targets P4HA1 [46]. The current study with CRC cells showed that miR-124 targets P4HA1 and decreases malignant phenotypes. Other miRNAs that regulate the function of P4HA1 are miR-122 in ovarian cancer cells [47] and miR-30e in hepatoma cells [12].

Our prior study showed that, in prostate cancers, MMP1 is a downstream target of P4HA1 [15]. MMP1 is involved in CRC progression and tumor growth [48–50]. In the present study, P4HA1 knockdown in CRC cells decreased the protein levels of MMP1. Additionally, CRC cells treated with diethyl-pythiDC showed lower levels of MMP1, suggesting that CRC progresses through P4HA1 via MMP1.

Hydroxylation of collagen proteins by collagen prolyl-4-hydroxylases is essential for their functional folding and stability. P4HA1 interacts with AGO2, a regulator of miRNA function and maturity, and regulates its function by hydroxylating it at proline 700, which leads to angiogenesis [37]. A mutation at proline 700 or a dysfunction of P4HA1 reduces the stability of AGO2 [38]. AGO2 is involved in tumorigenesis and is overexpressed in various carcinomas [37]. As observed in the present study, CRC cells treated with diethyl-pythiDC had low levels of AGO2, suggesting that P4HA1 is involved in CRC progression through modulation of AGO2.

P4HA2 is involved in the progression of breast cancer [51,52] and oral squamous cell carcinoma [53]; P4HB functions in hepatocellular carcinoma [54], diffuse gliomas [55], and gioblastoma multiforme [56]. As shown in the present study, there was, for CRCs, a correlation between levels of P4HA1 with P4HA2 and P4HB; when P4HA1 was depleted, P4HA2 and P4HB protein levels were decreased. Treatment of CRC cells with diethyl-pythiDC decreased the levels of P4HA2 and P4HB. These findings suggest that P4HA1 interacts with its other isoforms in the progression of CRCs.

In sum, this is the first report showing that overexpression of P4HA1 has a role in growth and metastasis of CRCs, particularly in dissemination of CRC cells. In animal models, inhibition of P4HA1 decreased metastases to liver and bone. Expression of P4HA1 was dependent on miR-124, and in CRCs, its overexpression was independent of tumor stage and patient race/ethnicity, age, or gender and p53 and MSI status. Treatment of CRC cells with an inhibitor of P4HA1, diethyl-pythiDC, decreased proliferation, invasion, and migration of cells and tumor growth in a PDX model. The present results also elucidated roles of EZH2 and miRNA-124 in regulating the expression of P4HA1 and the oncogenic function of P4HA1 through the expression of MMP1 and AGO2. They also indicate that P4HA1 represents as a therapeutic target and lay a foundation for clinical testing of diethyl-pythiDC for treatment of CRC.

Acknowledgements

This study was supported, in part, by grant 5U54CA118948 and institutional impact funds (U.M.) and R01CA157845 (S.V.). We thank Dr. Donald Hill for his editorial assistance, and we acknowledge the help provided by the Tissue Biorepository Facility and Preclinical Imaging Shared Facility (grant P30CA013148) to the O'Neal Comprehensive Cancer Center of UAB.

Appendix A. Supplementary data

Supplementary data to this article can be found online at https://doi.org/10.1016/j.tranon.2020.100754.

References

[1] RL Siegel, KD Miller, A Jemal, Cancer statistics, 2020, CA Cancer J Clin 70 (2020) 7–30.
[2] RR Huxley, A Ansary-Moghaddam, P Clifton, S Czernichow, CL Parr, M Woodward, The impact of dietary and lifestyle risk factors on risk of colorectal cancer: a quantitative overview of the epidemiological evidence, Int J Cancer 125 (2009) 171–180.
[3] L Liu, Y Zhang, CC Wong, J Zhang, Y Dong, X Li, W Kang, FKL Chan, JJY Sung, J Yu, RNF6 promotes colorectal cancer by activating the Wnt/beta-catenin pathway via ubiquitination of TLE3, Cancer Res 78 (2018) 1958–1971.
[4] EM Grasset, T Bertero, A Bozec, J Friard, I Bourget, S Pisano, M Lecacheur, M Maiel, C Bailleux, A Emelyanov, et al., Matrix stiffening and EGFR cooperate to promote the collective invasion of cancer cells, Cancer Res 78 (2018) 5229–5242.
[5] CJ Ko, CC Huang, HY Lin, CP Juan, SW Lan, HY Shyu, SR Wu, PW Hsiao, HP Huang, CT Shun, et al., Androgen-induced TMPRSS2 activates matriptase and promotes extracellular matrix degradation, prostate cancer cell invasion, tumor growth, and metastasis, Cancer Res 75 (2015) 2949–2960.
[6] NA van Huizen, RRJ Coebergh van den Braak, M Doukas, LJM Dekker, IJ JNM, TM Luider, Up-regulation of collagen proteins in colorectal liver metastasis compared with normal liver tissue, J Biol Chem 294 (2019) 281–289.
[7] SN Kehlet, R Sanz-Pamplona, S Brix, DJ Leeming, MA Karsdal, V Moreno, Excessive collagen turnover products are released during colorectal cancer progression and elevated in serum from metastatic colorectal cancer patients, Sci Rep 6 (2016) 30599.
[8] DM Gilkes, P Chaturvedi, S Bajpai, CC Wong, H Wei, S Pitcairn, ME Hubbi, D Wirtz, GL Semenza, Collagen prolyl hydroxylases are essential for breast cancer metastasis, Cancer Res 73 (2013) 3285–3296.
[9] J Myllyharju, Prolyl 4-hydroxylases, the key enzymes of collagen biosynthesis, Matrix Biol 22 (2003) 15–24.

[10] Y Zhou, G Jin, R Mi, J Zhang, J Zhang, H Xu, S Cheng, Y Zhang, W Song, F Liu, Knockdown of P4HA1 inhibits neovascularization via targeting glioma stem cell-endothelial cell transdifferentiation and disrupting vascular basement membrane, Oncotarget 8 (2017) 35877–35889.
[11] G Xiong, RL Stewart, J Chen, T Gao, TL Scott, LM Samayoa, K O'Connor, AN Lane, R Xu, Collagen prolyl 4-hydroxylase 1 is essential for HIF-1alpha stabilization and TNBC chemoresistance, Nat Commun 9 (2018) 4456.
[12] G Feng, H Shi, J Li, Z Yang, R Fang, L Ye, W Zhang, X Zhang, MiR-30e suppresses proliferation of hepatoma cells via targeting prolyl 4-hydroxylase subunit alpha-1 (P4HA1) mRNA, Biochem Biophys Res Commun 472 (2016) 516–522.
[13] A Atkinson, A Renziehausen, H Wang, C Lo Nigro, L Lattanzio, M Merlano, B Rao, L Weir, A Evans, R Matin, et al., Collagen prolyl hydroxylases are bifunctional growth regulators in melanoma, J Invest Dermatol 139 (2019) 1118–1126.
[14] XP Cao, Y Cao, WJ Li, HH Zhang, ZM Zhu, P4HA1/HIF1alpha feedback loop drives the glycolytic and malignant phenotypes of pancreatic cancer, Biochem Biophys Res Commun 516 (2019) 606–612.
[15] BV Chakravarthi, SS Pathi, MT Goswami, M Cieslik, H Zheng, S Nallasivam, SR Arekapudi, X Jing, J Siddiqui, J Athanikar, et al., The miR-124-prolyl hydroxylase P4HA1-MMP1 axis plays a critical role in prostate cancer progression, Oncotarget 5 (2014) 6654–6669.
[16] WM Hu, J Zhang, SX Sun, SY Xi, ZJ Chen, XB Jiang, FH Lin, ZH Chen, YS Chen, J Wang, et al., Identification of P4HA1 as a prognostic biomarker for high-grade gliomas, Pathol Res Pract 213 (2017) 1365–1369.
[17] M Kappler, J Kotrba, T Kaune, M Bache, S Rot, D Bethmann, H Wichmann, A Guttler, U Bilkenroth, S Horter, et al., P4HA1: a single-gene surrogate of hypoxia signatures in oral squamous cell carcinoma patients, Clin Transl Radiat Oncol 5 (2017) 6–11.
[18] DR Gawel, EJ Lee, X Li, S Lilja, A Matussek, S Schafer, RS Olsen, M Stenmarker, H Zhang, M Benson, An algorithm-based meta-analysis of genome- and proteome-wide data identifies a combination of potential plasma biomarkers for colorectal cancer, Sci Rep 9 (2019) 15575.
[19] BV Chakravarthi, MT Goswami, SS Pathi, M Dodson, DS Chandrashekar, S Agarwal, S Nepal, SA Hodigere Balasubramanya, J Siddiqui, RJ Lonigro, et al., Expression and role of PAICS, a de novo purine biosynthetic gene in prostate cancer, Prostate 77 (2017) 10–21.
[20] S Agarwal, S Saini, D Parashar, A Verma, N Jagadish, A Batra, S Suri, A Bhatnagar, A Gupta, AS Ansari, et al., Expression and humoral response of A-kinase anchor protein 4 in cervical cancer, Int J Gynecol Cancer 23 (2013) 650–658.
[21] S Agarwal, S Saini, D Parashar, A Verma, A Sinha, N Jagadish, A Batra, S Suri, A Gupta, AS Ansari, et al., The novel cancer-testis antigen A-kinase anchor protein 4 (AKAP4) is a potential target for immunotherapy of ovarian serous carcinoma, Oncoimmunology 2 (2013), e24270.
[22] N Jagadish, D Parashar, N Gupta, S Agarwal, S Purohit, V Kumar, A Sharma, R Fatima, AP Topno, C Shaha, et al., A-kinase anchor protein 4 (AKAP4) a promising therapeutic target of colorectal cancer, J Exp Clin Cancer Res 34 (2015) 142.
[23] BV Chakravarthi, MT Goswami, SS Pathi, AD Robinson, M Cieslik, DS Chandrashekar, S Agarwal, J Siddiqui, S Daignault, SL Carskadon, et al., MicroRNA-101 regulated transcriptional modulator SUB1 plays a role in prostate cancer, Oncogene 35 (2016) 6330–6340.
[24] B Chakravarthi, DS Chandrashekar, S Agarwal, SAH Balasubramanya, SS Pathi, MT Goswami, X Jing, R Wang, R Mehra, IA Asangani, et al., miR-34a regulates expression of the stathmin-1 oncoprotein and prostate cancer progression, Mol Cancer Res 16 (2018) 1125–1137.
[25] S Saini, S Agarwal, A Sinha, A Verma, D Parashar, N Gupta, AS Ansari, NK Lohiya, N Jagadish, A Suri, Gene silencing of A-kinase anchor protein 4 inhibits cervical cancer growth in vitro and in vivo, Cancer Gene Ther 20 (2013) 413–420.
[26] S. Agarwal, M. Behring, K. Hale, S. Al Diffalha, K. Wang, U. Manne, S. Varambally, MTHFD1L, A folate cycle enzyme, is involved in progression of colorectal cancer. Transl Oncol, 12 (2019) 1461–1467.
[27] N Jagadish, S Agarwal, N Gupta, R Fatima, S Devi, V Kumar, V Suri, R Kumar, V Suri, TC Sadasukhi, et al., Heat shock protein 70-2 (HSP70-2) overexpression in breast cancer, J Exp Clin Cancer Res 35 (2016) 150.
[28] D Kanojia, M Garg, S Saini, S Agarwal, D Parashar, N Jagadish, A Seth, A Bhatnagar, A Gupta, R Kumar, et al., Sperm associated antigen 9 plays an important role in bladder transitional cell carcinoma, PLoS One 8 (2013), e81348.
[29] A Sinha, S Agarwal, D Parashar, A Verma, S Saini, N Jagadish, AS Ansari, NK Lohiya, A Suri, Down regulation of SPAG9 reduces growth and invasive potential of triple-negative breast cancer cells: possible implications in targeted therapy, J Exp Clin Cancer Res 32 (2013) 69.
[30] B Chakravarthi, MDC Rodriguez Pena, S Agarwal, DS Chandrashekar, SA Hodigere Balasubramanya, FJ Jabboure, A Matoso, TJ Bivalacqua, K Rezaei, A Chaux, et al., A role for de novo purine metabolic enzyme PAICS in bladder cancer progression, Neoplasia 20 (2018) 894–904.
[31] N Jagadish, D Parashar, N Gupta, S Agarwal, V Suri, R Kumar, V Suri, TC Sadasukhi, A Gupta, AS Ansari, et al., Heat shock protein 70-2 (HSP70-2) is a novel therapeutic target for colorectal cancer and is associated with tumor growth, BMC Cancer 16 (2016) 561.
[32] S Kaiser, YK Park, JL Franklin, RB Halberg, M Yu, WJ Jessen, J Freudenberg, X Chen, K Haigis, AG Jegga, et al., Transcriptional recapitulation and subversion of embryonic colon development by mouse colon tumor models and human colon cancer, Genome Biol 8 (2007) R131.
[33] N. Cancer genome atlas, comprehensive molecular characterization of human colon and rectal cancer. Nature, 487 (2012) 330–337.
[34] DS Chandrashekar, B Bashel, SAH Balasubramanya, CJ Creighton, I Ponce-Rodriguez, B Chakravarthi, S Varambally, UALCAN: a portal for facilitating tumor subgroup gene expression and survival analyses, Neoplasia 19 (2017) 649–658.
[35] R Assi, D Mukherji, A Haydar, M Saroufim, S Temraz, A Shamseddine, Metastatic colorectal cancer presenting with bone marrow metastasis: a case series and review of literature, J Gastrointest Oncol 7 (2016) 284–297.
[36] JD Vasta, KA Andersen, KM Deck, CP Nizzi, RS Eisenstein, RT Raines, Selective inhibition of collagen prolyl 4-hydroxylase in human cells, ACS Chem Biol 11 (2016) 193–199.
[37] Z Ye, H Jin, Q Qian, Argonaute 2: a novel rising star in cancer research, J Cancer 6 (2015) 877–882.
[38] HH Qi, PP Ongusaha, J Myllyharju, D Cheng, O Pakkanen, Y Shi, SW Lee, J Peng, Y Shi, Prolyl 4-hydroxylation regulates argonaute 2 stability, Nature 455 (2008) 421–424.
[39] DM Gilkes, GL Semenza, D Wirtz, Hypoxia and the extracellular matrix: drivers of tumour metastasis, Nat Rev Cancer 14 (2014) 430–439.
[40] Q Liu, H Zhang, X Jiang, C Qian, Z Liu, D Luo, Factors involved in cancer metastasis: a better understanding to "seed and soil" hypothesis, Mol Cancer 16 (2017) 176.
[41] J Massague, AC Obenauf, Metastatic colonization by circulating tumour cells, Nature 529 (2016) 298–306.
[42] DM Burgenske, DJ Monsma, JP MacKeigan, Patient-derived xenograft models of colorectal cancer: procedures for engraftment and propagation, Methods Mol Biol 1765 (2018) 307–314.
[43] C Maletzki, S Bock, P Fruh, K Macius, A Witt, F Prall, M Linnebacher, NSG mice as hosts for oncological precision medicine, Lab Invest 100 (2020) 27–37.
[44] J Xia, Z Wu, C Yu, W He, H Zheng, Y He, W Jian, L Chen, L Zhang, W Li, miR-124 inhibits cell proliferation in gastric cancer through down-regulation of SPHK1, J Pathol 227 (2012) 470–480.
[45] YJ Liang, QY Wang, CX Zhou, QQ Yin, M He, XT Yu, DX Cao, GQ Chen, JR He, Q Zhao, MiR-124 targets Slug to regulate epithelial-mesenchymal transition and metastasis of breast cancer, Carcinogenesis 34 (2013) 713–722.
[46] XH Peng, HR Huang, J Lu, X Liu, FP Zhao, B Zhang, SX Lin, L Wang, HH Chen, X Xu, et al., MiR-124 suppresses tumor growth and metastasis by targeting Foxq1 in nasopharyngeal carcinoma, Mol Cancer 13 (2014) 186.
[47] Y Duan, Y Dong, R Dang, Z Hu, Y Yang, Y Hu, J Cheng, MiR-122 inhibits epithelial mesenchymal transition by regulating P4HA1 in ovarian cancer cells, Cell Biol Int 42 (2018) 1564–1574.
[48] R Bendardaf, A Buhmeida, R Ristamaki, K Syrjanen, S Pyrhonen, MMP-1 (collagenase-1) expression in primary colorectal cancer and its metastases, Scand J Gastroenterol 42 (2007) 1473–1478.
[49] AH Said, JP Raufman, G Xie, The role of matrix metalloproteinases in colorectal cancer, Cancers (Basel) 6 (2014) 366–375.
[50] L Herszenyi, I Hritz, G Lakatos, MZ Varga, Z Tulassay, The behavior of matrix metalloproteinases and their inhibitors in colorectal cancer, Int J Mol Sci 13 (2012) 13240–13263.
[51] G Xiong, L Deng, J Zhu, PG Rychahou, R Xu, Prolyl-4-hydroxylase alpha subunit 2 promotes breast cancer progression and metastasis by regulating collagen deposition, BMC Cancer 14 (2014) 1.
[52] MS Toss, IM Miligy, KL Gorringe, A AlKawaz, H Khout, IO Ellis, AR Green, EA Rakha, Prolyl-4-hydroxylase alpha subunit 2 (P4HA2) expression is a predictor of poor outcome in breast ductal carcinoma in situ (DCIS), Br J Cancer 119 (2018) 1518–1526.
[53] KP Chang, JS Yu, KY Chien, CW Lee, Y Liang, CT Liao, TC Yen, LY Lee, LL Huang, SC Liu, et al., Identification of PRDX4 and P4HA2 as metastasis-associated proteins in oral cavity squamous cell carcinoma by comparative tissue proteomics of microdissected specimens using iTRAQ technology, J Proteome Res 10 (2011) 4935–4947.
[54] W Xia, J Zhuang, G Wang, J Ni, J Wang, Y Ye, P4HB promotes HCC tumorigenesis through downregulation of GRP78 and subsequent upregulation of epithelial-to-mesenchymal transition, Oncotarget 8 (2017) 8512–8521.
[55] H Zou, C Wen, Z Peng, Y Shao, L Hu, S Li, C Li, HH Zhou, P4HB and PDIA3 are associated with tumor progression and therapeutic outcome of diffuse gliomas, Oncol Rep 39 (2018) 501–510.
[56] S Sun, D Lee, AS Ho, JK Pu, XQ Zhang, NP Lee, PJ Day, WM Lui, CF Fung, GK Leung, Inhibition of prolyl 4-hydroxylase, beta polypeptide (P4HB) attenuates temozolomide resistance in malignant glioma via the endoplasmic reticulum stress response (ERSR) pathways, Neuro Oncol 15 (2013) 562–577.